16. D.J. Kern, D.H. Werner, A. Monorchio, L. Lanuzza, and M.J. Wilhelm, The design synthesis of multiband artificial magnetic conductors using high impedance frequency selective surfaces, IEEE Trans Antennas Propag 53 (2005), 8–16.

WIDEBAND MONOPOLE ANTENNA COUPLED WITH A CHIP-INDUCTOR-LOADED SHORTED STRIP FOR LTE/WWAN MOBILE HANDSET

Shu-Chuan Chen and Kin-Lu Wong
Department of Electrical Engineering, National Sun Yat-sen University, Kaohsiung 80424, Taiwan; Corresponding author: wongkl@ema.ee.nsysu.edu.tw

Received 31 August 2010

ABSTRACT: *An eight-band long term evolution/wireless wide area network (LTE/WWAN) mobile handset antenna using a wideband monopole antenna coupled with a chip-inductor-loaded shorted strip is presented. Two wide operating bands are obtained to cover the eight-band LTE/WWAN operation in the 698–960 and 1710–2690 MHz bands. The antenna's lower band is contributed by the coupled shorted strip of length about 100 mm which is short-circuited to the system ground plane of the mobile handset through a loaded chip inductor of 10 nH. The loaded chip inductor leads to dual-resonant behavior of the excited resonant mode and greatly enhances the lower-band bandwidth. The upper band is formed by a wide resonant mode generated by the wideband monopole antenna and a higher-order resonant mode generated by the coupled shorted strip. The upper-band bandwidth of larger than 1 GHz is hence obtained. With two wide bands obtained, the antenna can be disposed on the bottom edge of the main circuit board of the mobile handset with a small board area of 10 × 60 mm^2. The specific absorption rate (SAR) values of the antenna for 1-g head tissue are also well below the limit of 1.6 W/kg for frequencies over the operating bands.*
 Microwave Opt Technol Lett 53:1293–1298, 2011; View this article online at wileyonlinelibrary.com. DOI 10.1002/mop.25977

Key words: *mobile antennas; internal handset antennas; LTE antennas; WWAN antennas; multiband antennas*

1. INTRODUCTION

To achieve wideband operation for the internal mobile handset antennas, the use of coupling feed, especially the printed distributed coupling feed [1–6], has been shown to be an effective technique in widening the bandwidth. This technique of using distributed coupling feed is generally applied to the shorted monopole antenna or planar inverted-F antennas. By using a distributed coupling feed, dual-resonance excitation for the antenna's lower band can be obtained [1–3], and widened bandwidth can hence be achieved. There are two reasons that the dual-resonance excitation for the antenna's lower band can be obtained. Firstly, the coupling feed can contribute additional capacitance to compensate for the large input inductance seen in the antenna's lower band at around 900 MHz. This can lead to an additional zero reactance occurred in the proximity of the existing zero reactance, that is, there can be two zero reactance or two resonances occurred in the desired 900 MHz band. Secondly, mainly owing to the long feeding and coupling strips in the distributed coupling feed, the input resistance level at around the two resonances, which is usually much larger than 50 Ω, can be significantly decreased. These two conditions result in a dual-resonance excitation with good impedance matching for the antenna's lower band. Hence, a wide lower band to cover the wireless wide area network (WWAN) operation in the GSM850/900 bands (824–960 MHz) can be obtained for the antenna. However, with such a distributed coupling feed design, the antenna's upper band is usually difficult to show a wide bandwidth of larger than 1 GHz to cover both the WWAN operation in the GSM1800/1900/UMTS bands (1710–2170 MHz) and the long term evolution (LTE) operation in the LTE2300/2500 bands (2300–2690 MHz) [7, 8].

In this article, we present a new wideband internal handset antenna design using a wideband monopole antenna coupled with a chip-inductor-loaded shorted strip. The obtained lower band shows a very wide bandwidth of larger than 300 MHz to cover not only the GSM850/900 bands (824–960 MHz) but also the LTE700 band (698–787 MHz). The obtained upper band shows an even wider bandwidth of larger than 1 GHz to easily cover the GSM1800/1900/UMTS/LTE2300/2500 bands (1710–2690 MHz). To achieve a wide upper band for the antenna, a wideband monopole antenna having a similar geometry to the ultra-wideband (UWB) planar monopole antenna [9–13] is used in the proposed design. The UWB planar monopole antenna replaces the simple feeding strip in the distributed coupling feed [1–6], which leads to a wide resonant mode excited in the desired upper band. Then, the wideband monopole antenna capacitively excites a chip-inductor-loaded shorted strip through a long coupling gap to generate a dual-resonance excitation in the desired lower band. This dual-resonance excitation effect is very similar to that obtained using the printed distributed coupling feed discussed above. Further, a higher-order resonant mode contributed by the chip-inductor-loaded shorted strip is excited to combine with the wide resonant mode generated by the wideband monopole antenna to form the desired upper band of bandwidth larger than 1 GHz. That is, the proposed antenna can provide two wide operating bands to cover the eight-band LTE/WWAN operation in the 698–960 and 1710–2690 MHz bands. Details of the proposed antenna mounted at the bottom edge of the main circuit board of the mobile handset are described in the article. Results of the proposed antenna including its SAR (specific absorption rate) values [14, 15] for 1-g head tissue are presented and discussed.

2. PROPOSED ANTENNA

Figure 1 shows the geometry of the proposed wideband monopole antenna coupled with a chip-inductor-loaded shorted strip for eight-band LTE/WWAN mobile handset application. Note that the antenna is placed at the bottom edge of the main circuit board of the mobile handset [16–20]. This arrangement can lead to decreased SAR values and is attractive for practical applications. The antenna can be disposed on a small no-ground board space of 10 × 60 mm^2 on the main circuit board, which in this study is an FR4 substrate of relative permittivity 4.4, loss tangent 0.02, and size 110 × 60 mm^2. Also, a ground plane of size 100 × 60 mm^2 is printed on the back surface of the FR4 substrate as the system ground plane of the mobile handset.

A plastic casing of relative permittivity 3.0, loss tangent 0.02, and thickness 1 mm is used to simulate the practical mobile handset casing which encloses the main circuit board including the antenna as shown in the figure. Note that the major portion of the antenna is printed on the main circuit board, with a small metal portion of width 3 mm bent to be perpendicular to the main circuit board to decrease the antenna footprint. The antenna hence shows a low profile of 3 mm above

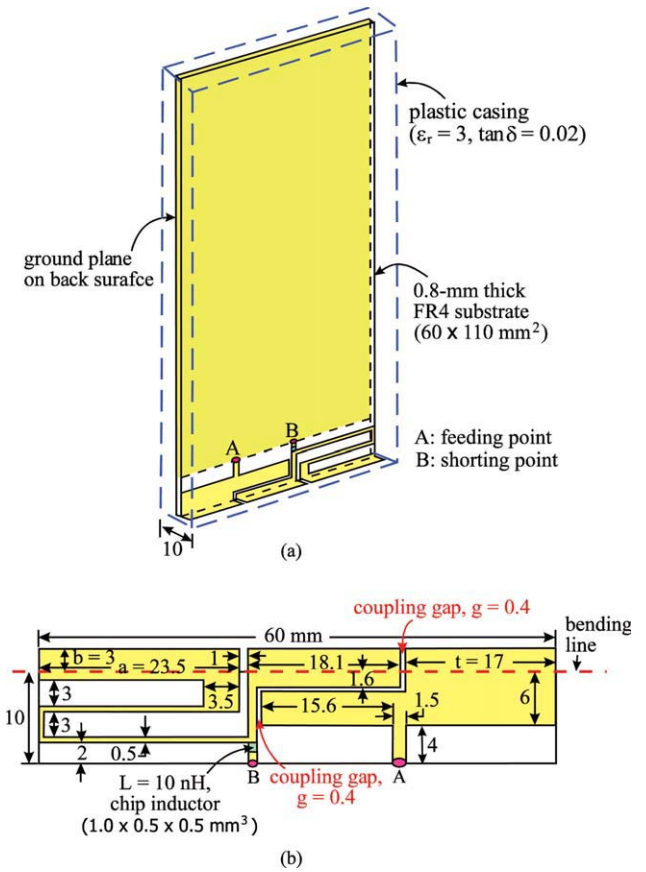

Figure 1 Geometry of the proposed wideband monopole antenna coupled with a chip-inductor-loaded shorted strip for eight-band LTE/WWAN mobile handset application. [Color figure can be viewed in the online issue, which is available at wileyonlinelibrary.com]

the main circuit board, which is attractive for thin mobile handset applications.

The antenna comprises a wideband monopole antenna as the driven element and a coupled chip-inductor-loaded shorted strip as the parasitic element. The wideband monopole antenna generally has a similar geometry to the traditional UWB planar monopole antenna [9–13], and the obtained bandwidth for the monopole antenna alone in this study can be larger than 700 MHz with the center frequency at about 2300 MHz. To decrease the size of the wideband monopole antenna in the proposed design, one corner of the monopole antenna is removed, which has small effects on the obtained bandwidth of the monopole antenna. With the removed corner, a longer boundary of the monopole antenna can be used to provide sufficient capacitive coupling to excite the shorted strip. In this case, the coupling gap (g) of width 0.4 mm has a length of about 26 mm.

The parasitic shorted strip is short-circuited through a chip inductor of 10 nH and a via-hole at point B (the shorting point) in the circuit board to the system ground plane on the back surface. The length of the shorted strip is about 100 mm, close to a quarter-wavelength at about 800 MHz. Through a long coupling gap (g) of width 0.4 mm, the quarter-wavelength monopole mode can be excited. This long coupling gap is similar to that in the long printed distributed coupling feed in [1–6]. Further, the loading chip inductor not only shifts the excited resonant modes to lower frequencies but also causes dual-resonance excitation of the excited quarter-wavelength monopole mode contributed by the shorted strip. The effect of shifting the excited resonant modes to lower frequencies is similar to

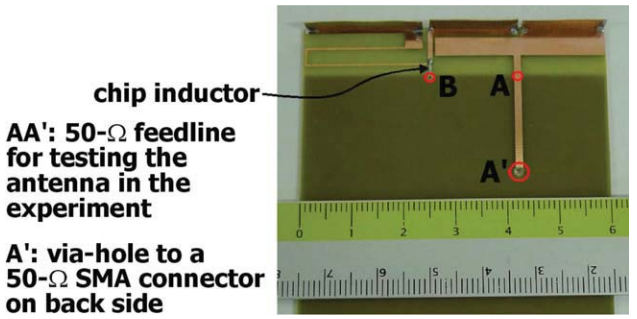

Figure 2 Photo of the fabricated antenna (plastic casing as handset casing is not included in the photo). [Color figure can be viewed in the online issue, which is available at wileyonlinelibrary.com]

that of the loaded chip inductor in the antennas reported in [21–28]. This is because the chip inductor provides additional inductance to compensate for the increased capacitance with decreased resonant length of the antenna. However, it is noted that by using the chip inductor to short-circuit the shorted strip to cause dual-resonance excitation for bandwidth enhancement has not yet been reported. This dual-resonance effect is a combined effect of the capacitive coupling excitation through the long coupling gap and the loaded chip inductor for short-circuiting. With the dual-resonance excitation, enhanced bandwidth for the antenna's lower band to cover the desired 698–960 MHz band is obtained.

Moreover, the shorted strip can generate a high-order resonant mode at about 1850 MHz, which combines with the wide resonant mode contributed by the wideband monopole antenna to form a wide upper band to cover the desired 1710–2690 MHz. With the wide lower and upper bands obtained, the antenna can cover eight-band LTE/WWAN operation. In this study, the antenna has been fabricated and tested. A photo of the fabricated antenna is shown in Figure 2. For testing the antenna in the experiment, a short 50-Ω microstrip feedline is printed on the front surface of the main circuit board. One end of the microstrip feedline is connected to point A (the feeding point of the antenna) and the other end is connected through a via-hole at point A′ in the circuit board to a 50-Ω SMA connector on the back side of the circuit board.

3. RESULTS AND DISCUSSION

Figure 3 shows the measured and simulated return loss of the proposed antenna. Two wide operating bands are obtained to

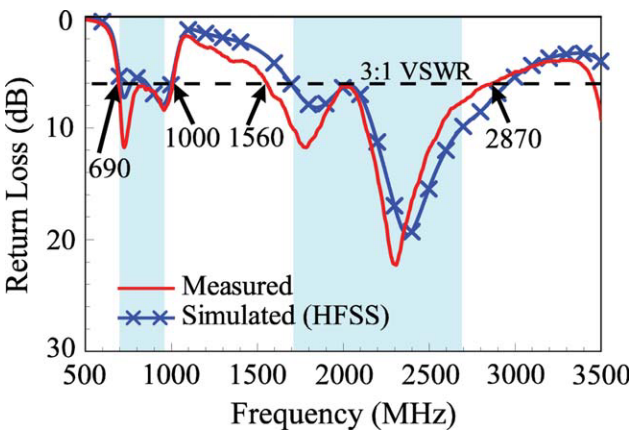

Figure 3 Measured and simulated return loss for the proposed antenna. [Color figure can be viewed in the online issue, which is available at wileyonlinelibrary.com]

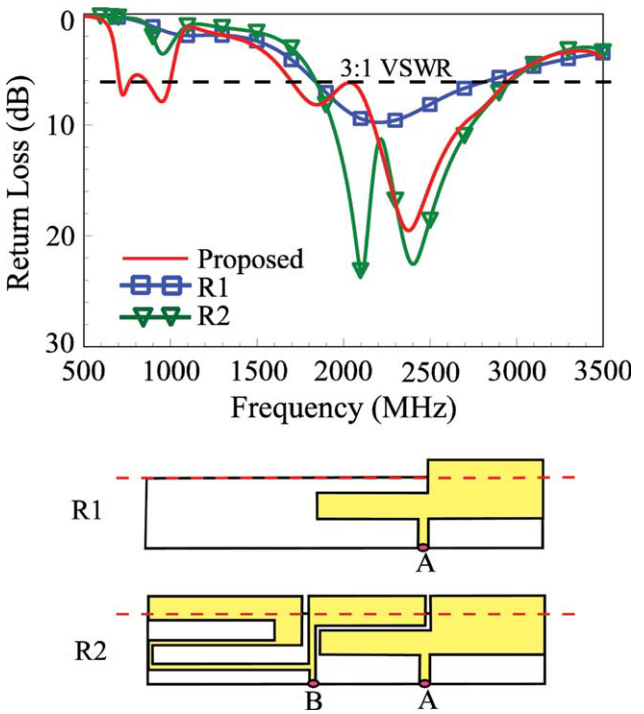

Figure 4 Simulated return loss for the proposed antenna, the case with the wideband monopole antenna only (R1), and the case without the loaded chip inductor in the coupled shorted strip (R2). [Color figure can be viewed in the online issue, which is available at wileyonlinelibrary.com]

cover the 698–960 and 1710–2690 MHz bands (see the two shaded frequency ranges in the figure) for LTE700/GSM850/900 and GSM1800/1900/UMTS/LTE2300/2500 operations, respectively. Agreement between the measurement and simulation is also obtained. The simulated results are obtained using commercial simulation software high frequency structure simulator [29]. Also note that the bandwidth definition of 3:1 VSWR (6-dB return loss) is widely used as the design specification for the internal mobile handset antennas for WWAN and LTE operations.

To analyze the operating principle of the antenna, Figure 4 shows the simulated return loss for the proposed antenna, the case with the wideband monopole antenna only (R1), and the case without the loaded chip inductor in the coupled shorted strip (R2). For R1, only a wide resonant mode centered at about 2300 MHz is generated. By adding a coupled shorted strip to the wideband monopole antenna (R2 shown in the figure), a resonant mode at about 1 GHz is excited, although its impedance matching is poor. By further using a chip-inductor-loaded shorting strip to replace the simple shorting strip in R2, the narrow resonant mode at about 1 GHz is shifted to lower frequencies and also shows improved impedance matching. This behavior can be seen more clearly in the simulated input impedance shown in Figure 5. Two resonances at about 800 and 1000 MHz with good impedance matching are hence obtained. This causes a dual-resonance excitation for the antenna's lower band and results in a much widened lower-band bandwidth to cover the 698–960 MHz band. In addition, an additional higher-order resonant mode at about 1850 MHz is generated to combine with the wide resonant mode contributed by the wideband monopole antenna to form a very wide upper band to cover the 1710–2690 MHz band.

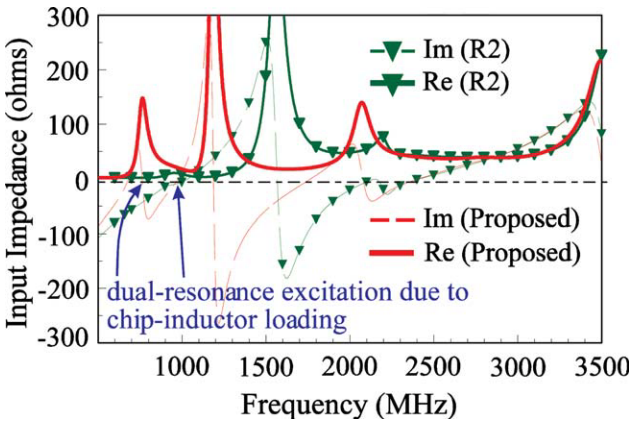

Figure 5 Simulated input impedance for the proposed antenna and the case without the loaded chip inductor in the coupled shorted strip (R2) studied in Figure 4. [Color figure can be viewed in the online issue, which is available at wileyonlinelibrary.com]

A parametric study is also conducted. Figure 6 shows the simulated return loss as a function of the length a and width b of the end section in the coupled shorted strip. Other dimensions are the same as in Figure 1. Results for the length a varied from

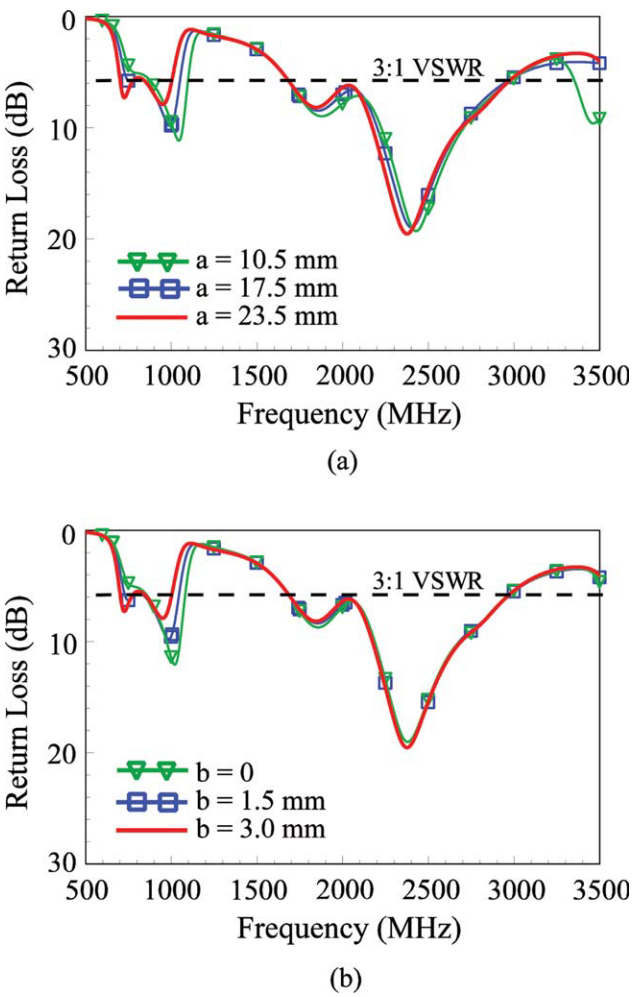

Figure 6 Simulated return loss as a function of (a) the end-section length a and (b) the end-section width b in the coupled shorted strip. Other dimensions are the same as in Figure 1. [Color figure can be viewed in the online issue, which is available at wileyonlinelibrary.com]

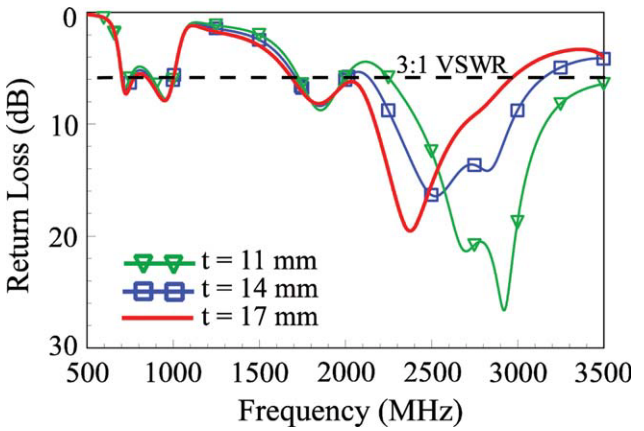

Figure 7 Simulated return loss as a function of the width t in the wideband monopole antenna. Other dimensions are the same as in Figure 1. [Color figure can be viewed in the online issue, which is available at wileyonlinelibrary.com]

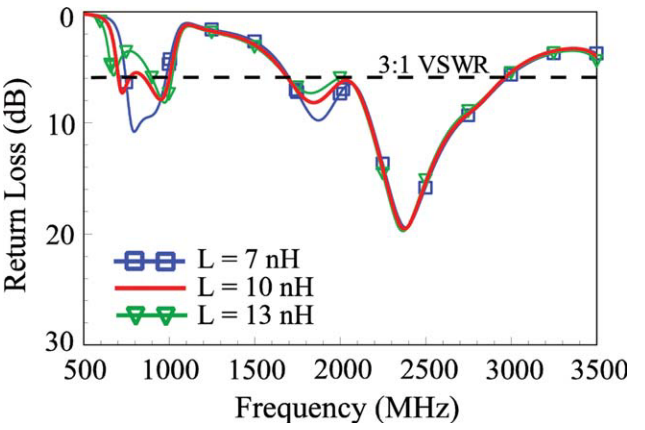

Figure 9 Simulated return loss as a function of the inductance L of the loaded chip inductor. Other dimensions are the same as in Figure 1. [Color figure can be viewed in the online issue, which is available at wileyonlinelibrary.com]

10.5 to 23.5 mm are presented in Figure 6(a). Since the shorted strip contributes to the generation of the dual-resonant mode in the lower band, a decrease in the length a shifts the center frequency of the dual-resonant mode to higher frequencies. This agrees with the expectation, and hence the length a can be used to adjust the occurrence of the dual-resonant mode to cover the desired lower band. At the same time, some slight variations on the impedance matching of the frequencies in the upper band are also seen. However, the obtained upper-band bandwidth is about the same.

Results for the width b varied from 0 to 3.0 mm are shown in Figure 6(b). Similar to the effects seen for the length a in Figure 6(a), by varying the width b, the occurrence of the dual-resonance mode can be adjusted. Results indicate that by selecting the width b to be 3.0 mm in this study, the desired 698–960 MHz band can be obtained.

Figure 7 shows the simulated return loss as a function of the width t in the wideband monopole antenna. Other dimensions are the same as in Figure 1. Strong effects on the second mode in the upper band are seen. This confirms that this wide resonant mode is contributed mainly by the wideband monopole antenna, and by varying the length t, the occurrence of this wide resonant mode can be adjusted. It is also interesting to note that other resonant modes are very slightly affected by the length t. This makes the respective tuning of the excited resonant modes in the proposed antenna easy to achieve.

Figure 8 shows the simulated return loss as a function of the coupling-gap width g between the wideband monopole antenna and the coupled shorted strip. Very small or no effects on the resonant modes in the upper band are seen, while there are relatively large effects on the dual-resonant mode in the lower band. This is also an attractive feature, since it makes the respective tuning of the excited resonant modes in the proposed antenna easy to achieve.

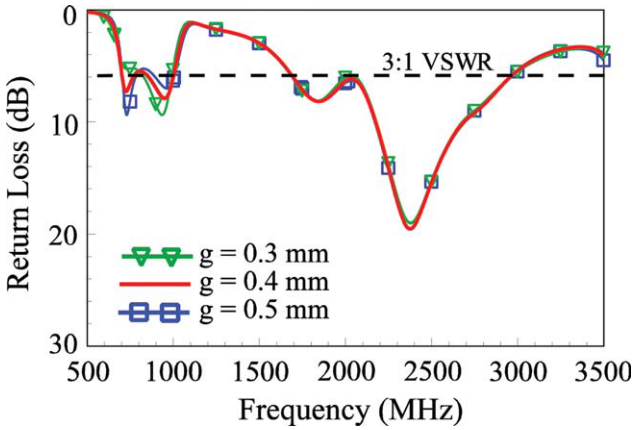

Figure 8 Simulated return loss as a function of the coupling-gap width g between the wideband monopole antenna and the coupled shorted strip. [Color figure can be viewed in the online issue, which is available at wileyonlinelibrary.com]

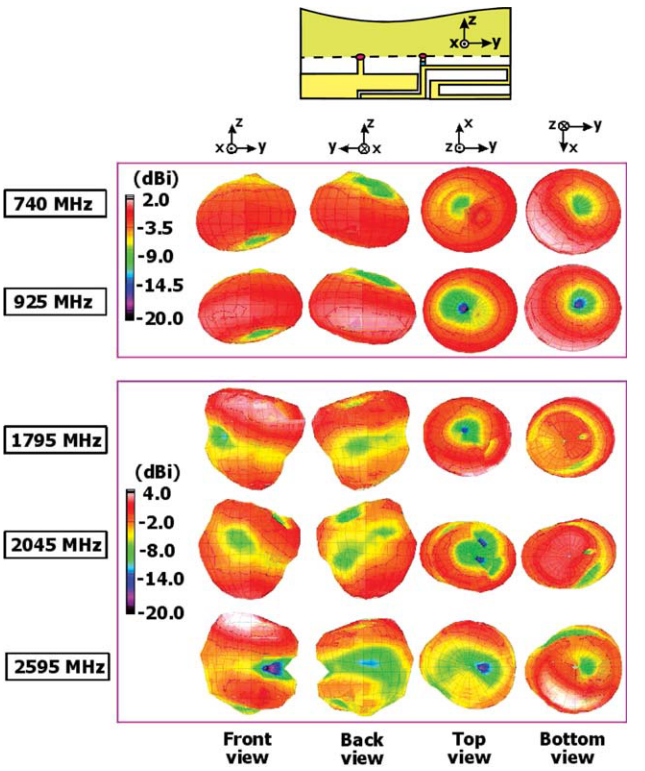

Figure 10 Measured three-dimensional total-power radiation patterns for the fabricated antenna. [Color figure can be viewed in the online issue, which is available at wileyonlinelibrary.com]

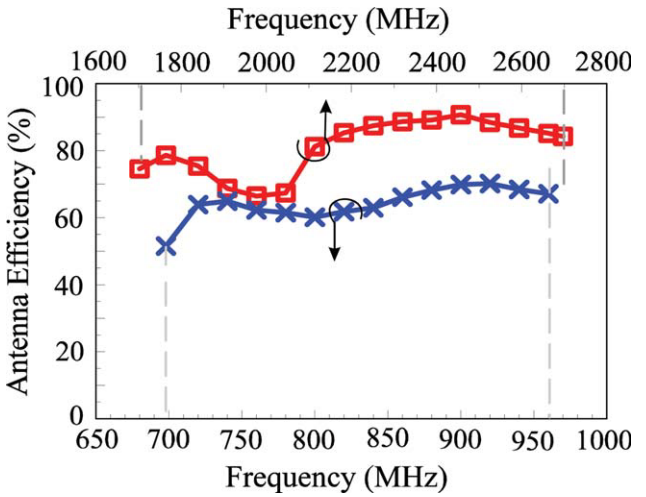

Figure 11 Measured antenna efficiency (mismatching loss included) for the fabricated antenna. [Color figure can be viewed in the online issue, which is available at wileyonlinelibrary.com]

Figure 9 shows the simulated return loss as a function of the inductance L of the loaded chip inductor. Results for the inductance L varied from 7 to 13 nH are presented. Strong effects are seen in the dual-resonant mode in the lower band, while the obtained upper-band bandwidths are about the same. This is also reasonable, since the loaded chip inductor leads to the occurrence of the dual-resonant mode in the lower band.

Measured radiation characteristics of the fabricated antenna are also studied. Figure 10 shows the measured three-dimensional total-power radiation patterns for the fabricated antenna. The radiation patterns are measured in a far-field anechoic chamber, and measured results at typical frequencies are presented. At each frequency, four radiation patterns seen in four different directions are shown. At 740 and 925 MHz in the lower band, the radiation patterns are close to those of the traditional half-wavelength dipole antenna. Omnidirectional radiation in the azimuthal plane (x-y plane) is generally obtained. At 1795, 2045, and 2595 MHz in the upper band, some nulls or dips are seen in the azimuthal plane for the measured radiation patterns, which are close to those of the traditional higher-order resonant modes of the dipole antenna. These results are similar to those of the traditional internal WWAN handset antennas [30]. The measured antenna efficiency (mismatching loss included) for the fabricated antenna is presented in Figure 11. The antenna efficiency ranges from about 50–70% in the lower band and about 66–90% in the upper band. With the antenna efficiency better than 50% over the operating bands, it is good for practical handset applications.

The SAR results are also studied. Figure 12 shows the SAR simulation model and the simulated SAR values for 1-g head tissue. The SAR simulation model is provided by SEMCAD X version 14 [31]. The input power and return loss at the testing frequencies are also given in the table shown in the figure. As explained earlier, the antenna is attractive to be mounted at the bottom edge of the handset to obtain decreased SAR values. For all the testing frequencies, the obtained SAR values are all less than 1.6 W/kg, which is the limit for 1-g head tissue [14]. This indicates that the proposed antenna is acceptable for practical handset applications.

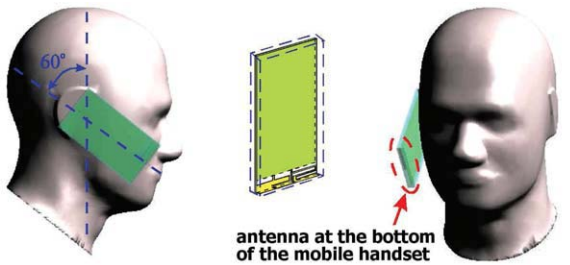

Frequency (MHz)	740	859	925	1795	1920	2045	2350	2595
1-g SAR (W/kg)	0.45	1.16	1.32	0.73	0.55	0.30	0.69	0.61
Input power (Watt in dBm)	21	24	24	21	21	21	21	21
Return loss (dB)	9.0	9.1	11.2	9.7	7.8	5.6	19.0	10.5

Figure 12 SAR simulation model and the simulated SAR values for 1-g head tissue. [Color figure can be viewed in the online issue, which is available at wileyonlinelibrary.com]

4. CONCLUSION

An eight-band LTE/WWAN mobile handset antenna has been proposed. A new design technique for achieving two wide operating bands to cover eight-band LTE/WWAN operation has been presented. The antenna uses a driven wideband monopole antenna to generate a wide resonant mode for the upper band and a parasitic shorted strip to generate a dual-resonant mode for the lower band. The latter is obtained by further applying a chip-inductor-loaded shorting strip to replace the simple shorting strip in the parasitic shorted strip, and the obtained lower-band bandwidth can be larger than 300 MHz. The chip-inductor-loaded shorted strip also contributes a higher-order resonant mode to combine with the wide resonant mode generated by the wideband monopole antenna to achieve the desired upper band of bandwidth larger than 1 GHz. In addition to the wideband operation obtained, the antenna occupies a small board space of 10×60 mm^2 and thin thickness of 3 mm on the main circuit board. The antenna also shows good far-field radiation characteristics and acceptable SAR values (less than 1.6 W/kg for 1-g head tissue), making it very promising for practical handset applications.

REFERENCES

1. K.L. Wong and C.H. Huang, Bandwidth-enhanced internal PIFA with a coupling feed for quad-band operation in the mobile phone, Microwave Opt Technol Lett 50 (2008), 683–687.
2. K.L. Wong and C.H. Huang, Printed PIFA with a coplanar coupling feed for penta-band operation in the mobile phone, Microwave Opt Technol Lett 50 (2008), 3181–3186.
3. C.H. Chang and K.L. Wong, Internal coupled-fed shorted monopole antenna for GSM850/900/1800/1900/UMTS operation in the laptop computer, IEEE Trans Antennas Propagat 56 (2008), 3600–3604.
4. K.L. Wong and S.J. Liao, Uniplanar coupled-fed printed PIFA for WWAN operation in the laptop computer, Microwave Opt Technol Lett 51 (2009), 549–554.
5. C.H. Chang, K.L. Wong, and J.S. Row, Coupled-fed small-size PIFA for penta-band folder-type mobile phone application, Microwave Opt Technol Lett 51 (2009), 18–23.
6. C.T. Lee and K.L. Wong, Uniplanar coupled-fed printed PIFA for WWAN/WLAN operation in the mobile phone, Microwave Opt Technol Lett 51 (2009), 1250–1257.
7. C.T. Lee and K.L. Wong, Planar monopole with a coupling feed and an inductive shorting strip for LTE/GSM/UMTS operation in

the mobile phone, IEEE Trans Antennas Propagat 58 (2010), 2479–2483.
8. K.L. Wong, W.Y. Chen, C.Y. Wu, and W.Y. Li, Small-size internal eight-band LTE/WWAN mobile phone antenna with internal distributed LC matching circuit, Microwave Opt Technol Lett 52 (2010), 2244–2250.
9. K.L. Wong, S.W. Su, and Y.L. Kuo, Printed ultra-wideband diversity monopole antenna, Microwave Opt Technol Lett 38 (2003), 257–259.
10. K.L. Wong, C.H. Wu, and S.W. Su, Ultra-wideband square planar metal-plate monopole antenna with a trident-shaped feeding strip, IEEE Trans Antennas Propagat 53 (2005), 1262–1269.
11. Z.N. Chen, M.J. Ammann, and M.Y.W. Chia, Broadband square annular planar monopoles, Microwave Opt Technol Lett 36 (2003), 449–454.
12. N.P. Agrawall, G. Kumar, and K.P. Ray, Wide-band planar monopole antennas, IEEE Trans Antennas Propagat 46 (1998), 294–295.
13. Z.N. Low, J.H. Cheong, and C.L. Law, Low-cost PCB antenna for UWB applications, IEEE Antennas Wireless Propagat 4 (2005), 237–239.
14. American National Standards Institute (ANSI), Safety levels with respect to human exposure to radio-frequency electromagnetic field, 3 kHz to 300 GHz, ANSI/IEEE standard C95.1, April 1999.
15. W. Yu, S. Yang, C.L. Tang, and D. Tu, Accurate simulation of the radiation performances of a mobile slide phone in a hand-head position, IEEE Antennas Propagat Mag 52 (2010), 168–177.
16. C.H. Chang and K.L. Wong, Printed λ/8-PIFA for penta-band WWAN operation in the mobile phone, IEEE Trans Antennas Propagat 57 (2009), 1373–1381.
17. S.C. Chen and K.L. Wong, Bandwidth enhancement of coupled-fed on-board printed PIFA using bypass radiating strip for eight-band LTE/GSM/UMTS slim mobile phone, Microwave Opt Technol Lett 52 (2010), 2059–2065.
18. C.H. Chang and K.L. Wong, Bandwidth enhancement of internal WWAN antenna using an inductively coupled plate in the small-size mobile phone, Microwave Opt Technol Lett 52 (2010), 1247–1253.
19. K.L. Wong and C.H. Chang, On-board small-size printed monopole antenna integrated with USB connector for penta-band WWAN mobile phone, Microwave Opt Technol Lett 52 (2010), 2523–2527.
20. Y.W. Chi and K.L. Wong, Quarter-wavelength printed loop antenna with an internal printed matching circuit for GSM/DCS/PCS/UMTS operation in the mobile phone, IEEE Trans Antennas Propagat 57 (2009), 2541–2547.
21. K.L. Wong and S.C. Chen, Printed single-strip monopole using a chip inductor for penta-band WWAN operation in the mobile phone, IEEE Trans Antennas Propagat 58 (2010), 1011–1014.
22. T.W. Kang and K.L. Wong, Very-small-size printed monopole with embedded chip inductor for 2.4/5.2/5.8 GHz WLAN laptop computer antenna, Microwave Opt Technol Lett 52 (2010), 171–177.
23. C.H. Chang and K.L. Wong, Small-size printed monopole with a printed distributed inductor for penta-band WWAN mobile phone application, Microwave Opt Technol Lett 51 (2009), 2903–2908.
24. T.W. Kang and K.L. Wong, Chip-inductor-embedded small-size printed strip monopole for WWAN operation in the mobile phone, Microwave Opt Technol Lett 51 (2009), 966–971.
25. J. Thaysen and K.B. Jakobsen, A size reduction technique for mobile phone PIFA antennas using lumped inductors, Microwave J 48 (2005), 114–126.
26. S.H. Yeh and K.L. Wong, Dual-band PIFA with a chip inductor-loaded spiral strip, Microwave Opt Technol Lett 33 (2002), 394–397.
27. J. Carr, Antenna toolkit, 2nd ed., Newnes, UK, 2001, pp. 111–112.
28. T.H. Chang and J.F. Kiang, Meshed antenna reduction by embedding inductors, In: 2005 IEEE AP-S International Symp and USNC/URSI Nat Radio Sci Meeting, Washington, DC, 2005, Session 78.
29. http://www.ansoft.com/products/hf/hfss/, Ansoft Corporation HFSS.
30. K.L. Wong, Planar antennas for wireless communications, Wiley, New York, 2003.
31. http://www.semcad.com, SEMCAD, Schmid & Partner Engineering AG (SPEAG).

DESIGN OF A NEW UWB-INTEGRATED ANTENNA FILTER WITH A REJECTED WLAN BAND AT 5.8 GHz

A. Djaiz,[1] M. Nedil,[1] M. A. Habib,[2] and T. A. Denidni[2]
[1] University of Québec in Abitibi-Témiscamingue, Val-d'Or, QC, Canada J9P 1S2; Corresponding author: Azzeddine.Djaiz@uqat.ca
[2] INRS-EMT, University of Québec, Montréal, QC, Canada, H5A 1K6

Received 6 September 2010

ABSTRACT: *In this article, a new ultra-wideband (UWB)-integrated antenna-filter notched at HiPerLAN 5.8 GHz frequency is presented. This antenna filter system is composed of a rectangular slot fed with a microstrip rectangular patch by coupling effect and cascaded with an UWB interdigital hairpin resonator filter. The proposed components, antenna and filter, are matched with 50 Ω, to allow an easier connection, with no need to add additional matching circuit. To improve the selectivity of the antenna filter system, two wide sections of microstrip line was inserted between the input/output feed lines and the interdigital hairpin resonators of the UWB filter. To validate the proposed concept, a prototype was fabricated and tested. The experimental results are presented and discussed. The obtained results show a good agreement between experimental and full-wave electromagnetic (EM) simulation results.* © 2011 Wiley Periodicals, Inc.
Microwave Opt Technol Lett 53:1298–1302, 2011; View this article online at wileyonlinelibrary.com. DOI 10.1002/mop.25963

Key words: *planar circuits; ultra-wideband systems; notched antenna; interdigital filter*

1. INTRODUCTION

Since the release by the Federal Communication Commission (FCC) of the band 3.1 to 10.6 GHz, the ultra-wideband (UWB) communication system have been developed widely and rapidly advancing as high data rate wireless communication technology. To fitful these issue, several UWB antenna designs have been proposed [1–3]. However, the band reserved for narrow band systems such as, high performance local area network (HiPerLAN) at 5.8 GHz should be notched to avoid interference between the both systems. Accordingly, and to resolve this problem, some works to notch the HiPerLAN frequency band have been reported and widely discussed [2–8]. A common approach is to use UWB monopole with different shapes [2, 3]. Other techniques have also been investigated such as, the insertion of the split-ring slot resonator, the U-shaped slot resonant structure, or stubs [4, 5]. Lee et al. [6] have proposed to perturb matching impedance and create an open circuit at the undesired frequency. Recently, UWB filters with a notched band have been proposed to reject any undesired band by using different techniques. The most effectives techniques is to include the insertion of embedded open-circuited stub into the UWB antenna [7], or integrating split ring resonators in the active region of filter [8].

In this article, we present a new UWB integrated filter antenna. This configuration allows obtaining low interference at 5.8 GHz, reduced size, high performances in terms of radiation patterns stability, and the characteristics of the UWB system. The antenna is a rectangular slot fed by a coupling microstrip